NANO LETTERS

2001
Vol. 1, No. 10
551−556

Shell-Tunneling Spectroscopy of the Single-Particle Energy Levels of Insulating Quantum Dots

E. P. A. M. Bakkers,[†] Z. Hens,[†] A. Zunger,[‡] A. Franceschetti,[‡] L. P. Kouwenhoven,[§] L. Gurevich,[§] and D. Vanmaekelbergh[†]

Debye Institute, University of Utrecht, P.O. Box 80000, 3508 TA Utrecht, The Netherlands, National Renewable Energy Laboratory, Golden, Colorado 80401, and Department of Applied Physics and ERATO Mesoscopic Correlation Project, Delft University of Technology, P.O. Box 5046, 5600 GA Delft, The Netherlands

Received June 20, 2001; *Revised Manuscript Received July 31, 2001*

ABSTRACT

The energy levels of CdSe quantum dots are studied by scanning tunneling spectroscopy. By varying the tip−dot distance, we switch from "shell-filling" spectroscopy (where electrons accumulate in the dot and experience mutual repulsion) to "shell-tunneling" spectroscopy (where electrons tunnel, one at a time, through the dot). Shell-tunneling spectroscopy provides the single-particle energy levels of the CdSe quantum dot. The results of both types of tunneling spectroscopy are compared with pseudopotential many-body calculations.

1. Introduction. Insulating nanocrystals with diameters in the 1−10 nm range might play an important role in future optical and electrical devices. Consequently, significant research is directed toward better control of the size, shape, and surface chemistry[1−3] of colloidal nanocrystals. In parallel, the interest in the electronic structure of these nanocrystals is rapidly increasing. Pseudopotential and tight-binding methods have been used to calculate the single-particle energy levels and many-body excitation spectra of a number of nanocrystals, such as InAs and InP,[4,5] CdSe,[6] Ge,[7] and Si.[8] Experimentally, the electronic structure of colloidal nanocrystals has been studied mostly via light absorption and emission spectroscopy.[9,10] Such experiments have revealed discrete excitonic transitions coupling valence holes with conduction electrons, demonstrating quantum confinement effects. It has, however, proven to be difficult to fully determine the individual electron and hole energy levels of insulating quantum dots by optical spectroscopy, since such experiments measure inherently electron + hole excitations, not the individual states.[11] In contrast, resonant tunneling spectroscopy provides a direct method to study the individual energy levels of nanocrystalline quantum dots. This is possible with a transistor-type configuration[12,13] or by using an STM. In the latter case, the tip is located above a nanocrystal, attached to an atomically flat substrate, forming a double-barrier tunnel junction (Figure 1). The tunnel current

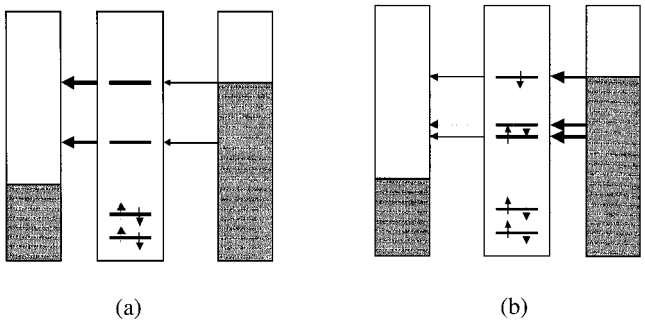

Figure 1. Schemes presenting the principles of resonant shell-tunneling and shell-filling spectroscopy. Electrons tunnel from the tip electrode (right-hand side), via the orbitals of the quantum dot (center) to the substrate electrode (left-hand side), as indicated by arrows. (a) *Shell-tunneling spectroscopy*: the tip is retracted from the dot, so that tunneling from the tip into the dot is much slower (thin arrows) than tunneling from the dot to the substrate (thick arrows): electrons tunnel one at the time through the device, electron−electron interactions do not occur. (b): *Shell-filling spectroscopy*: the tip is brought closer to the dot, so that tunneling from the tip into the dot (thick arrows) is much faster than tunneling out of the dot (thin arrows). The electrons accumulate in the dot, and the degeneracy of the states is broken by electron−electron Coulomb interactions.

I is measured as a function of the bias V, which is the difference in the electrochemical potentials of the tip and substrate electrode: $V = \mu_e^{tip} - \mu_e^{substrate}$. In this work, we use scanning tunneling spectroscopy to determine the single-particle electron levels and Coulomb repulsion energies in a colloidal CdSe quantum dot (diameter 4.3 ± 0.4 nm).

* Corresponding author. E-mail: Daniel@phys.uu.nl.
[†] University of Utrecht.
[‡] National Renewable Energy Laboratory.
[§] Delft University of Technology.

10.1021/nl015572b CCC: $20.00
Published on Web 08/30/2001

Electron−electron Coulomb interactions in the quantum dot may have a profound effect on the tunneling spectra. Resonant tunneling spectra depend sensitively on whether a carrier tunnels through an otherwise empty dot where interelectronic interactions are absent or whether carriers are accumulated inside the dot where interelectronic interactions occur, resulting in additional peaks. These limiting scenarios are decided by the dynamics of electron tunneling in to and out of the quantum dot.[14,15] Consider, for instance, resonant tip-to-dot-to-substrate tunneling occurring at positive bias ($V > 0$). At the first resonance the probability to find one electron in the LUMO of the quantum dot is

$$P(s^1) = \frac{2\Gamma_s^{in}}{2\Gamma_s^{in} + \Gamma_s^{out}} \quad (1)$$

in which Γ_s^{in} stands for the rate at which an electron with given spin tunnels from the tip into the empty s orbital, and Γ_s^{out} for the rate of tunneling from the occupied s orbital into the substrate electrode.

In the "shell-tunneling" case $\Gamma_s^{in} \ll \Gamma_s^{out}$; therefore, $P(s^1) \cong 0$, and a single electron tunnels through the nanodevice at the time. Tunneling leads to polarization of the dot by a single electron (i.e., dielectric solvation,[16] which depends on the dielectric discontinuity $\epsilon_{in} - \epsilon_{out}$ between the dot and its environment), but Coulomb interactions between two (or more) additional electrons do not occur (see Figure 1a). This still holds when the electrochemical potential of the tip electrode is increased further, such that tunneling from the tip to the second level (a p-type level) also occurs. In this type of *shell-tunneling* spectroscopy, the peaks in the conductance spectrum correspond to the single-particle energy levels, with their attendant degeneracies (two for s, six for p).

In the "shell-filling" case $\Gamma_s^{in} \gg \Gamma_s^{out}$; therefore, $P(s^1) \cong 1$, and the s orbital will be occupied with a single electron at the first resonance. When μ_e^{tip} is further increased, a second resonance will occur, corresponding to the filling of the s orbital with a second electron (see Figure 1b). The energy difference between the first and second resonance corresponds to the electron−electron Coulomb energy in the s orbital. The third resonance corresponds to the occupation of a p orbital with one electron while the s orbital is doubly occupied. Thus, *shell-filling* spectroscopy corresponds to a more complex spectrum, in which the degeneracy of the orbitals is lifted due to electron−electron Coulomb interactions. Recently, shell-filling spectra of InAs quantum dots have been presented, showing that the first electron orbital (LUMO) is an s-type double degenerate orbital, and the second orbital is a 6-fold degenerate p-type orbital.[17,18]

In this Letter, we demonstrate that electron−electron Coulomb interactions can be turned on and off by controlling the tunneling dynamics in the substrate/Q-dot/tip device. We present results obtained with CdSe quantum dots, 4.3 ± 0.4 nm in diameter, attached to a Au(111) substrate, via a *rigid* sulfur-terminated oligo(cyclohexylidene) SAM layer. In this way, the dot/substrate distance is kept constant at 0.8 nm.[19]

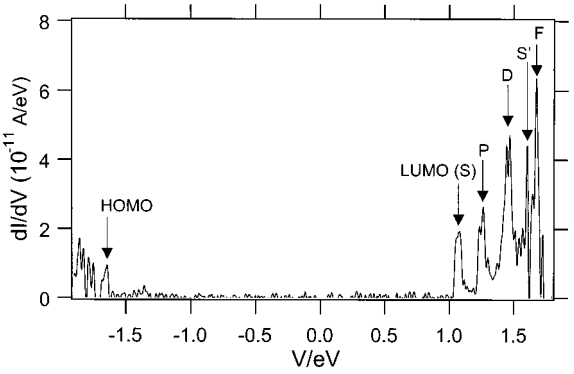

Figure 2. Shell-tunneling spectrum of a 4.3 nm CdSe quantum dot (4.2 K, set point 5×10^{-12} A at 1.4 eV, estimated tip−dot distance 1.4 nm[22]). The five peaks in the positive bias range ($V >$ 1 eV) correspond to tunneling through the electron orbitals; according to pseudopotential theory the orbitals are (in order of increasing energy) s-type (LUMO), p-type, d-type, s′-type, and f-type. The peaks in the negative bias range ($V < -1.6$ eV) correspond to tunneling through the HOMO and other lower lying hole states. The zero-conductivity gap corresponds to the quasiparticle gap of the quantum dot.

We vary the width of the dot/tip tunneling barrier and show that the relative rates of tip-to-dot and dot-to-substrate tunneling critically determines the electron occupation in the CdSe dot. If the tip is sufficiently retracted, electrons tunnel one at a time through the tip/quantum dot/gold device, and *shell-tunneling* spectra are acquired. When the tip is brought closer to the dot, the spectra become more complex, indicating partial *shell-filling*. The peaks in the tunneling spectra are assigned with the aid of Monte Carlo simulations of the electron occupation in the CdSe quantum dot. As a result, the electron−electron interaction energy can be distinguished from the single-particle energy separations between the orbitals. We compare the measured energy separation between individual levels and the interelectronic Coulomb interactions with the results of pseudopotential calculations.[20]

2. Spectra. In Figure 2, a typical conductance spectrum is presented for a 4.3 ± 0.4 nm CdSe quantum dot under conditions that the tip is relatively far retracted from the dot. In a previous study[21] we showed that under these conditions, a change of the bias leads merely to a change of the tip Fermi level with respect to the energy levels in the dot (details of the bias distribution across the tip/dot and dot/substrate barrier are given below[22]). A zero conductivity gap is found between 1 and −1.6 eV bias. Negative of −1.6 eV, several small conductance peaks can be seen, corresponding to tunneling through the first valence orbitals (hole states) of the CdSe quantum dot. In the bias range more positive than 1 eV, five peaks are found, increasing in height with increasing energy. The tunneling spectra become unstable at a bias exceeding 1.7 eV. Tunneling spectra acquired with other 4.3 ± 0.4 nm CdSe quantum dots under the same conditions show the same features. We infer that the spectrum shown in Figure 2 is a shell-tunneling spectrum; this will be validated by the analysis given below.

Figure 3 shows a typical spectrum in the positive bias range, obtained with a 12 times higher set-point current than

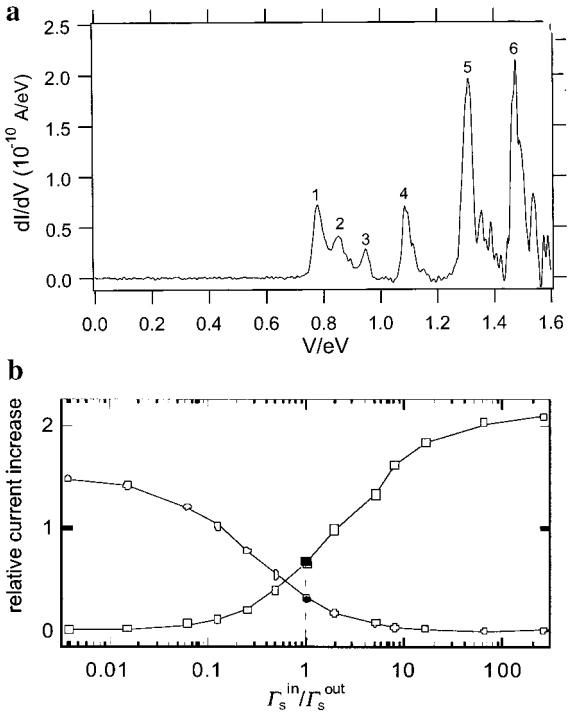

Figure 3. (a) Spectrum (at 4.2 K) of a 4.3 nm CdSe quantum dot in the positive bias range obtained with a smaller tip−dot distance than in Figure 2: set point 60×10^{-12} A at a bias of 1.4 eV; estimated tip−dot distance 0.8 nm.[22] This spectrum is acquired under conditions of *partial shell-filling*: tip-to-s orbital tunneling (into the dot) is as fast as tunneling from the s orbital to the substrate (out of the dot).[22] The peaks correspond to resonant tip-to-dot-to-substrate tunneling with zero, one, or two additional electrons in the quantum dot. An assignment of the peaks is given in the text. (b) Ratios of the current increase of the second vs first (□) and the third vs first (○) resonance as a function of the ratio $\Gamma_s^{in}/\Gamma_s^{out}$ quantifying the relative tunneling rates in to and out of the quantum dot. The results are obtained with Monte Carlo simulations. The first, second, and third resonance correspond to the transitions $s^0 \rightarrow s^1$, $s^1 \rightarrow s^2$, and $s^0p^0 \rightarrow s^0p^1$, respectively, and to peaks 1, 2, and 3 in Figure 3a. The left-hand side, with $\Gamma_s^{in}/\Gamma_s^{out} \ll 1$, corresponds to *shell-tunneling* spectroscopy ($s^1 \rightarrow s^2$ absent); the right-hand side, with $\Gamma_s^{in}/\Gamma_s^{out} \gg 1$, to shell-filling spectroscopy ($s^0p^0 \rightarrow s^0p^1$ absent). The ratio of the peak intensities observed in Figure 3a (black marks) shows that $\Gamma_s^{in} = \Gamma_s^{out}$ in this experimental situation.

used to acquire the shell-tunneling spectrum in Figure 2. This means that the tip has been brought closer to the dot and that the ratio of the rates of tunneling into vs out of the dot is considerably increased. Under these conditions we first find three closely spaced peaks, *decreasing* in intensity. There is also some additional structure (i.e., small satellites) close to peaks 5 and 6. The occurrence of closely spaced peaks indicates the breakdown of the spin and orbital degeneracy due to electron−electron Coulomb interactions in the CdSe quantum dot. In other words, more than one electron is present in the dot at a given time. This is validated by the results acquired at even smaller tip−dot distances (larger set-point currents) showing a large number of closely spaced peaks. We infer that the results presented in Figure 3 reflect (partial) shell-filling.

3. Interpretation of "Shell-Filling" Spectra (Figure 3). We simulated the (*I*, *V*) tunneling spectra of CdSe quantum dots using a Monte Carlo algorithm. We used as input a scheme for the single-particle orbitals predicted from pseudopotential theory;[20] this means in order of increasing energy: the first orbital is s-type, the second orbital is p-type, the third orbital is d-type, the fourth orbital is s-type (denoted as s′), and the fifth orbital is f-type. We assume a substrate/dot/tip double-barrier tunnel junction with one-dimensional barriers; the width of the dot−substrate barrier is constant, the width of the tip−dot barrier can be varied. This mimics the experimental conditions. For a given value of the electrochemical potential of the tip (source) electrode with respect to the energy level system we monitor the state transitions in the quantum dot and the current using a stochastic sequence of 10^5 resonant electron tunneling steps via the electron energy levels of the dot. By repeating this procedure for a wide range of tip electrochemical potentials, the *I*−*V* relationship is simulated for a given structure of the junction. (Injection of holes in the valence levels is not possible here due to the large HOMO−LUMO gap of the CdSe quantum dot, and the asymmetric distribution of the bias over both tunneling barriers.) Comparison of the simulated and experimental spectra enables us to assign the peaks in the experimental spectra unambiguously. We found that the spectrum of Figure 3 is acquired under conditions where tunneling into the dot is as fast as tunneling out of the dot,[22] thus reflecting *partial* shell-filling. Table 1 shows the assignment of the peaks in terms of specific transitions between two states of the quantum dot. The transitions change the occupation of the electron levels; the valence hole levels remain fully occupied. The third column gives the theoretical chemical potential for the transitions. In Table 2, we present the charging energies, i.e., the differences between the chemical potentials of Table 1. The pseudopotential values for the model CdSe quantum dot[20] are given in the third column. The experimental separations between the peaks, averaged over four CdSe quantum dots (4.3 ± 0.4 nm) [and corrected for $V_{tip-dot}/V = 0.84$[22]] are given in the fourth column.

Table 1. State Transitions in the CdSe Quantum Dot Corresponding to the Peaks in the Partial Shell-Filling Spectrum (Figure 3)[a]

peak number	transition type	chemical potential
1	$s^0p^0 \rightarrow s^1p^0$	$\epsilon_s + \Sigma_s$
2	$s^1p^0 \rightarrow s^2p^0$	$\epsilon_s + \Sigma_s + J_{s-s}$
3	$s^0p^0 \rightarrow s^0p^1$	$\epsilon_p + \Sigma_p$
4	$s^2p^0 \rightarrow s^2p^1$	$\epsilon_p + \Sigma_p + 2J_{s-p} - K_{s-p}$
5	$s^2d^0 \rightarrow s^2d^1$	$\epsilon_d + \Sigma_d + 2J_{s-d} - K_{s-d}$
6	$s^2s'^0 \rightarrow s^2s'^1$	$\epsilon_{s'} + \Sigma_{s'} + 2J_{s-s'} - K_{s-s'}$

[a] The state transitions involve the electron levels (LUMO s, second level p, third level d, fourth level s′) while the valence levels are fully occupied. The third column gives the chemical potentials of the state transitions; ϵ_I stands for the energy of electron level *I*, Σ_I for the polarization energy of an electron in orbital *I*, J_{I-J} for the Coulomb repulsion energy between an electron in level *I* and an electron in level *J*, and K_{I-J} for the exchange energy between two electrons with parallel spins.

It follows from Table 2 that the energy difference between peak 2 and peak 1 is equal to the Coulomb energy between the two electrons in the s-orbital J_{s-s}. The calculations[20] give J_{s-s} = 280, 180, and 80 meV for ϵ_{out} = 2, 4, and 20,

Table 2. Charging Energies, i.e., Differences between the Chemical Potentials Given in Table 1[a]

pair of transitions	charging energy	pseudopotential value	exptl value (from partial shell-filling)
(2,1)	J_{s-s}	80[b]	60 ± 5
(3,1)	$(\epsilon_p - \epsilon_s) + (\Sigma_p - \Sigma_s) \cong (\epsilon_p - \epsilon_s)$	231	145 ± 8
(4,3)	$2J_{s-p} - K_{s-p} \cong 2J_{s-p}$	130[b]	120 ± 10
(5,4)	$(\epsilon_d - \epsilon_p) + (\Sigma_d - \Sigma_p) + 2(J_{s-d} - J_{s-p}) - (K_{s-d} - K_{s-p}) \cong (\epsilon_d - \epsilon_p)$	248	175 ± 10
(6,5)	$(\epsilon_{s'} - \epsilon_d) + (\Sigma_{s'} - \Sigma_d) + 2(J_{s-s'} - J_{s-d}) - (K_{s-s'} - K_{s-d}) \cong (\epsilon_{s'} - \epsilon_d)$	131	140 ± 17

[a] The third column gives the pseudopotential values (meV) calculated for the model quantum dot.[20] [b] Repulsion energies are calculated by assuming that the dielectric constant of the environment, ϵ_{out}, is 20. The fourth column gives the experimental values obtained from partial shell-filling spectra (Figure 3) measured with four 4.3 nm CdSe quantum dots.

respectively. The measured values, obtained with a number of 4.3 ± 0.4 nm CdSe dots, give $\Delta_{2,1} = 60 \pm 5$ meV, thus agreeing with the calculated values at high ϵ_{out}. The energy difference between peaks 4 and 3 is $2J_{s-p} - K_{s-p}$. Since the exchange energy is much smaller than the electron−electron Coulomb energy this amounts approximately to $2J_{s-p}$. The pseudopotential calculated value is 550, 350, and 130 meV for $\epsilon_{out} = 2$, 4, and 20, respectively. Analysis of the spectra obtained with a number of quantum dots gives 120 ± 10 meV. Interpretation of the experimental electron−electron repulsion energies with pseudopotential theory shows that under the conditions under which the shell-filling spectra were acquired, ϵ_{out} is in the range 20−25. Thus, the Coulomb repulsion energy between two electrons in the s orbital or in the s and p orbitals are strongly screened. It should be noted here that Klein et al. also found a relatively low value of 15 meV for the hole−hole Coulomb interaction energy in a 5.5 nm CdSe quantum dot, mounted via alkanedithiols between two gold electrodes.[13] Our results and those of Klein suggest that metal electrodes close to the dot (dot−electrode distance <1 nm) give rise to a relative high value for the effective dielectric constant ($\epsilon_{out} = 20-25$) of the immediate environment of the dot.

From partial shell-filling spectra, such as the one shown in Figure 3, it is also possible to obtain the energy separation between the electron levels. The charging energy between peak 3 and 1 is nearly equal to $\epsilon_p - \epsilon_s$, since $(\epsilon_p - \epsilon_s) \gg (\Sigma_p - \Sigma_s)$. Similarly, the peak separations (5,4) and (6,5) are close to $\epsilon_d - \epsilon_p$ and $\epsilon_{s'} - \epsilon_d$, respectively ($J_{s-d} \cong J_{s-p}$, $K \cong 0$). The energy separations between the electron levels are discussed in the next section.

4. Interpretation of "Shell-Tunneling" Spectra. We next interpret the results obtained with the tip retracted from the dot (estimated tip−dot distance close to 1.4 nm[22]). Under these conditions, tunneling from the tip into the dot is much slower than tunneling out of the dot to the substrate;[22] hence the spectra (such as the one shown in Figure 2) are shell-tunneling spectra.

(i) Electron Energy Levels. The peaks at positive bias correspond to tunneling through the *electron orbitals* of the CdSe dot, s, p, d, s′, and f-type in order of increasing energy. The current steps increase in height with increasing energy, reflecting the increasing spatial extension of the orbitals. Table 3 presents the transitions between the ground state and the different one-electron excited states, corresponding to the peaks in the shell-tunneling spectra at positive bias. Since the differences in the charging energies $\Sigma_J - \Sigma_I$ are much smaller than the energy differences between the electron levels $\epsilon_J - \epsilon_I$, the separations between the peaks in the shell-tunneling spectra are nearly equal to the energy separations between the electron levels s, p, d, s′, and f. The experimentally observed energy separations in millielectronvolts (corrected for $\Delta\mu_e^{tip}/V = 0.9$[22]) obtained with four CdSe quantum dots are presented in Table 4, together with the calculated values for a 4.7 nm model quantum dot. The energy separations between the single-particle levels obtained

Table 3. State Transitions in the CdSe Quantum Dot Corresponding to the Peaks at Positive Bias in the Shell-Tunneling Spectrum (Figure 2)[a]

peak symbol	transition type	chemical potential
LUMO (S)	$s^0 \rightarrow s^1$	$\epsilon_s + \Sigma_s$
p	$s^0p^0 \rightarrow s^0p^1$	$\epsilon_p + \Sigma_p$
d	$s^0d^0 \rightarrow s^0d^1$	$\epsilon_d + \Sigma_d$
s′	$s^0s'^0 \rightarrow s^0s'^1$	$\epsilon_{s'} + \Sigma_{s'}$
f	$s^0f^0 \rightarrow s^0f^1$	$\epsilon_f + \Sigma_f$

[a] The state transitions occur between the ground state and one-electron excited states. The chemical potentials $\epsilon_I + \Sigma_I$ of the state transitions are presented in the third column; ϵ_I is the energy of the electron level I, Σ_I is the charging energy due to one electron in level I.

Table 4. Energy Separations (meV) between the Electron Levels of a CdSe Quantum Dot Calculated from Pseudopotential Theory Compared to the Values Obtained from Shell-Tunneling and Partial Shell-Filling Spectroscopy[a]

separations	theory	shell-tunneling	(partial) shell-filling
$\epsilon_p - \epsilon_s$	231	173 ± 13	145 ± 8
$\epsilon_d - \epsilon_p$	248	188 ± 15	175 ± 10
$\epsilon_{s'} - \epsilon_d$	131	144 ± 15	140 ± 17
$\epsilon_f - \epsilon_{s'}$	101	87 ± 18	
quasiparticle gap	2480 (for $\epsilon_{out} = 2$)	2440 ± 80	
electron−hole Coulomb energy	290 (for $\epsilon_{out} = 2$)	290	

[a] The quasi-particle gap and electron−hole Coulomb energy are also presented. The calculations[20] were performed on a 4.7 nm dot which comes closest to the experimentally investigated dots of 4.3 ± 0.4 nm. The electron−hole Coulomb energy is obtained from the difference between the quasiparticle gap (from shell-tunneling spectroscopy) and the optical gap (from light absorption spectroscopy). Further details are given in section 4.

from the partial shell-filling spectra (see foregoing section) are also given.

The experimental separations follow the trend predicted by pseudopotential theory. For instance, $\epsilon_d - \epsilon_p$ is larger than $\epsilon_p - \epsilon_s$, in agreement with the prediction. Quantitatively, the experimental separations between the second and first, and between the third and second, are significantly smaller than the pseudopotential values for $\epsilon_p - \epsilon_s$ and $\epsilon_d - \epsilon_p$, respectively, while the experimental separations between the fourth and third, and fifth and fourth peak, are in good agreement with the predicted values of $\epsilon_{s'} - \epsilon_d$, and $\epsilon_f - \epsilon_{s'}$. Possible reasons for the discrepancies between theory and experiment find their origin in a number of experimental uncertainties. The first uncertainty is related to the size distribution of the CdSe nanocrystals (4.3 nm ± 10%) leading to ± 20% uncertainties in the energy-differences between the energy levels. The second uncertainty is related to the shape: it is not possible to detect small deviations from a spherical shape "in situ" with STM.

(ii) Quasiparticle Gap, Optical Gap, and HOMO−LUMO Gap. The first conductance peak in Figure 2 at *negative* bias corresponds to tunneling of a hole through the HOMO $\mu_h[s^o/s^1] = \epsilon_s^h - \Sigma_s^h$ ($\Sigma_s^h > 0$). The first peak at positive bias corresponds to tunneling of an electron through the LUMO $\mu_e[s^o/s^1] = \epsilon_s + \Sigma_s$. The zero-conductivity gap $\epsilon_g^{qp} = \mu_e[s^o/s^1] - \mu_h[s^o/s^1]$ (also called the "quasi-particle gap") of the quantum dot thus corresponds to the sum of the LUMO−HOMO single-particle gap $\epsilon_g^o = \epsilon_s - \epsilon_s^h$ plus the sum of self-polarization energies $\Sigma_s^e + \Sigma_s^h$ due to an electron in the LUMO and (separately) a hole in the HOMO. Pseudopotential theory predicts a (ϵ_{out} independent) value of $\epsilon_g^o = 2.21$ eV for the LUMO−HOMO single-particle gap for the 4.7 nm CdSe model quantum dot. The self-polarization energies of the incoming electron and hole depend sensitively on the effective dielectric constant of the immediate environment of the quantum dot.[16] For an effective dielectric constant of $\epsilon_{out} = 2$, pseudopotential theory predicts a value of $\Sigma_s = 0.147$ and $\Sigma_s^h = 0.125$ eV. This gives a calculated quasi-particle gap of $\epsilon_g^{qp} = 2.21 + (0.147 + 0.125) = 2.48$ eV. Measuring the zero-conductivity gap of four CdSe quantum dots with diameter 4.3 ± 0.4 nm (corrected for $\Delta\mu_e^{tip}/V = 0.9$) gives $\epsilon_g^{qp} = 2.44 \pm 0.08$ eV, in agreement with the predicted pseudopotential theory value for $\epsilon_{out} = 2$. For comparison, we predict ϵ_g^{qp} of 2.30 and 2.08 eV for $\epsilon_{out} = 4$ and 20, respectively.

The optical gap ϵ_g^{opt} differs from the quasi particle gap ϵ_g^{qp} by the electron−hole Coulomb attraction energy[16] $\epsilon_g^{opt} = \epsilon_g^{qp} - J_{e,h}$. The measured optical band gap of the 4.3 ± 0.4 nm CdSe colloids is 2.15 ± 0.05 eV, as determined from the first peak in the absorption spectrum. The calculated value is 2.19 eV for $\epsilon_{out} = 2$. We determine the electron−hole Coulomb energy $J_{e,h}$ from the difference $\epsilon_g^{qp} - \epsilon_g^{opt}$ and find a measured value of 0.29 eV, in excellent agreement with the pseudopotential value (also 0.29 eV) predicted for the dot imbedded in a dielectric with a dielectric constant of 2. These results highlight the differences between the HOMO−LUMO single particle gap $\epsilon_g^o = 2.21$ eV, the quasi particle gap $\epsilon_g^{qp} = 2.44$ eV, and the optical gap $\epsilon_g^{opt} = 2.15$ eV. Comparison between the experimental shell-tunneling spectra and pseudopotential theory shows that the effective dielectric constant around the quantum dot is close to 2, when the tip is retracted from the dot (estimated distance 1.4 nm[22]).

5. Summary. We have analyzed the resonant tunneling spectra obtained with an STM probing 4.3 nm CdSe quantum dots attached to a gold substrate via a rigid cyclohexylidene SAM of 0.8 nm width. The average population of a dot by electrons depends sensitively on the relative rates of tunneling in to and out of the dot. By retracting the tip sufficiently far from the dot, electrons tunnel one at a time through the orbitals of the quantum dot. The corresponding shell-tunneling spectra show the quasi-particle gap, and the energy separations between the first five single-particle electron levels of the CdSe quantum dot. There is a fair agreement with the single-electron energy-level spectrum calculated with pseudopotential theory. When the tip is closer to the dot, we observe partial "shell-filling". The spectra become more complex due to the effect of Coulomb interactions between the additional electrons in the dot. The strongly screened electron−electron repulsion energy obtained from the spectra can be understood with many-body pseudopotential calculations of interelectronic interactions.

Acknowledgment. Work at NREL was supported by the U.S. Department of Energy, SC-BES-DMS, under condensed matter. Z.H. acknowledges the FWO-Vlaanderen for a postdoctoral fellowship.

References

(1) Alivisatos, A. P. *J. Phys. Chem.* **1996**, *100*, 13226−13239.
(2) Weller, H. *Adv. Mater. (Weinheim, Fed. Repub. Ger.)* **1993**, *5*, 88−95.
(3) Talapin, D. V.; Rogach, A. L.; Kornowski, A.; Haase, M.; Weller, H. *Nano Lett.* **2001**, *1*, 207−211.
(4) Williamson, A. J.; Zunger, A. *Phys. Rev. B: Condens. Matter Mater. Phys.* **2000**, *61*, 1978−1991.
(5) Franceschetti, A.; Zunger, A. *Phys. Rev. B: Condens. Matter Mater. Phys.* **2000**, *62*, 2614−2623.
(6) Wang, L.-W.; Zunger, A. *Phys. Rev. B: Condens. Matter* **1996**, *53*, 9579−9582.
(7) Niquet, Y. M.; Allan, G.; Delerue, C.; Lannoo, M. *Appl. Phys. Lett.* **2000**, *77*, 1182−1184.
(8) Niquet, Y. M.; Delerue, C.; Allan, G.; Lannoo, M. *Phys. Rev. B: Condens. Matter Mater. Phys.* **2000**, *62*, 5109−5116.
(9) Empedocles, S. A.; Bawendi, M. G. *Science (Washington, D.C.)* **1997**, *278*, 2114−2117.
(10) Micic, O. I.; Jones, K. M.; Cahill, A.; Nozik, A. J. *J. Phys. Chem. B* **1998**, *102*, 9791−9796.
(11) Norris, D. J.; Bawendi, M. G. *Phys. Rev. B: Condens. Matter* **1996**, *53*, 16338−16346.
(12) Tarucha, S.; Austing, D. G.; Honda, T.; van der Hage, R. J.; Kouwenhoven, L. P. *Phys. Rev. Lett.* **1996**, *77*, 3613−3616.
(13) Klein, D. L.; Roth, R.; Lim, A. K. L.; Alivisatos, A. P.; McEuen, P. L. *Nature (London)* **1997**, *389*, 699−701.
(14) Averin, D. V.; Korotkov, A. N.; Likharev, K. K. *Phys. Rev. B−Condens. Matter* **1991**, *44*, 6199−6211.
(15) Su, B.; Goldman, V. J.; Cunningham, J. E. *Phys. Rev. B−Condens. Matter* **1992**, *46*, 7644−7655.
(16) Franceschetti, A.; Williamson, A.; Zunger, A. *J. Phys. Chem. B* **2000**, *104*, 3398−3401.
(17) Banin, U.; Cao, Y.; Katz, D.; Millo, O. *Nature (London)* **1999**, *400*, 542−544.
(18) Millo, O.; Katz, D.; Cao, Y.; Banin, U. *Phys. Rev. B: Condens. Matter Mater. Phys.* **2000**, *61*, 16773−16777.
(19) Bakkers, E. P. A. M.; Marsman, A. W.; Jenneskens, L. W.; Vanmaekelbergh, D. *Angew. Chem., Int. Ed. Engl.* **2000**, *39*, 2297−2299.

(20) *Pseudopotential calculations*: We considered theoretically a faceted and surface-passivated nearly spherical CdSe quantum dot with a diameter of 4.7 nm. This model quantum dot comes closest to those investigated experimentally. The single-particle electron and hole levels are first calculated using a plane-wave-basis with a nonlocal pseudopotential, as described in refs 5, 6, and 16. In the second step, the pseudopotential wave functions are used to compute the screened ($\epsilon_{in} = 6.8$) interelectronic Coulomb (*J*) and exchange (*K*) integrals, as well as the polarization energies (Σ), as a function of the dielectric constant of the immediate environment around the dot, ϵ_{out}, as described in ref 16. Pseudopotential calculations show that the polarization and Coulomb interaction energies for a given quantum dot depend strongly on ϵ_{out}.

(21) Bakkers, E. P. A. M.; Vanmaekelbergh, D. *Phys. Rev. B: Condens. Matter Mater. Phys.* **2000**, *62*, R7743−R7746.

(22) *Estimation of the tunneling rates and the structure of the tip/dot/substrate double-barrier tunnel junction.* It follows from our simulations that the respective current increase due to the second and third resonance, relative to the first, provides a sensitive fingerprint to derive the relative rates of tip-to-s-orbital tunneling vs s-to-substrate tunneling. Figure 3b covers the entire range from shell-tunneling (left-hand side) to shell-filling (right-hand side). The ratios of the intensities of peak 2 vs 1, and peak 3 vs 1 observed in the tunneling spectrum of Figure 3 are indicated with marks; we find $\Gamma_s^{in} \cong \Gamma_s^{out}$ (with an uncertainty of ±10%). We use this information to derive the characteristics of the substrate/spacer/Q-CdSe//tip junction. From the tunnel current corresponding to the transition $s^0 \rightarrow s^1$ [$I = 2e\Gamma_s^{out}\Gamma_s^{in}/(\Gamma_s^{out} + 2\Gamma_s^{in})$] we derive that $\Gamma_s^{in} = \Gamma_s^{out} = 0.2\ 10^9$/s. We assume that, since tunneling into the dot is as fast as tunneling out of the dot, the tip−dot distance is equal to the dot−substrate distance. The rigid cyclohexylidene spacer molecule determines the latter: thus substrate−dot distance = tip−dot distance = 0.8 nm (for Figure 3). In this simple approach, we do not account for the differences in the three-dimensional geometry and the variation in height of the tunneling barriers between the tip and dot, and dot and substrate. Using a value of 5.42 for the dielectric constant of the cyclohexylidene layer (obtained from electrochemical capacitance measurements), we estimate that $V_{tip/dot}/V = 0.84$. When the tip is retracted (spectrum of Figure 2), the current corresponding to the first resonance gives $\Gamma_s^{in} = 9\ 10^6$/s; thus $\Gamma_s^{in}/\Gamma_s^{out} = (9\ 10^6/0.2\ 10^9) = 1/22$. This ratio is sufficiently small to ensure that the spectrum in Figure 2 corresponds a *shell-tunneling* spectrum, acquired under conditions in which electrons tunnel one at the time through the device, without electron−electron interactions. From the ratio Γ_s^{in}(Figure 2)/Γ_s^{in}(Figure 3) = 1/22, it follows that the tip−dot distance under shell-tunneling conditions is close to 1.4 nm. We estimate that under conditions where we acquired shell-tunneling spectra, $V_{tip/dot}/V = 0.90$; this means that 90% of the bias is distributed over the tip−dot barrier. We should remark here that the derivation of the relative tunneling rates is exact, while the estimation of the tunneling distances and thus the ratio of the barrier capacitances depends (slightly) on the estimated barrier height.

NL015572B